Quenched mesonic spectrum at large N

Luigi Del Debbio

  SUPA, School of Physics and Astronomy, University of Edinburgh
  Edinburgh EH9 3JZ, Scotland,*
  and *Isaac Newton Institute for Mathematical Sciences*
  20 Clarkson Road, Cambridge CB3 0EH, UK
  E-mail: `luigi.del.debbio@ed.ac.uk`

Biagio Lucini

  Physics Department, Swansea University
  Singleton Park, Swansea SA2 8PP, UK*,
  and *Isaac Newton Institute for Mathematical Sciences*
  20 Clarkson Road, Cambridge CB3 0EH, UK
  E-mail: `b.lucini@swansea.ac.uk`

Agostino Patella

  Scuola Normale Superiore, Piazza dei Cavalieri 27, 56126 Pisa, Italy
  and INFN Pisa, Largo B. Pontecorvo 3 Ed. C, 56127 Pisa, Italy
  E-mail: `agostino.patella@sns.it`

Claudio Pica

  Physics Department, Brookhaven National Lab
  Upton, NY 11973-5000, USA
  E-mail: `pica@bnl.gov`

ABSTRACT: We compute the masses of the π and of the ρ mesons in the quenched approximation on a lattice with fixed lattice spacing $a \simeq 0.145$ fm for SU(N) gauge theory with $N = 2, 3, 4, 6$. We find that a simple linear expression in $1/N^2$ correctly captures the features of the lowest-lying meson states at those values of N. This enables us to extrapolate to $N = \infty$ the behaviour of m_π as a function of the quark mass and of m_ρ as a function of m_π. Our results for the latter agree within 5% with recent predictions obtained in the AdS/CFT framework.

KEYWORDS: Lattice Gauge Theory, Large N, Meson Spectrum.

---

*Permanent address.

Contents

1. Introduction

The theory of strong interactions, Quantum Chromodynamics (QCD), is a SU(3) gauge theory with n_f flavors of fermionic matter fields in the fundamental representation of the color group. For sufficiently small n_f, QCD displays many interesting non–perturbative phenomena, which are not captured by the conventional expansion in powers of the coupling constant. However, if we consider a SU(N) gauge theory, with a generic number of colors N, in the limit where N becomes large, the perturbative expansion can be reorganized in powers of $1/N$, and the contribution of each diagram can be directly related to its topology [1, 2]. The leading contribution in this expansion is given by planar diagrams, and a simple power counting argument suggests that corrections are $\mathcal{O}(1/N^2)$ in a pure gauge theory, while the fermionic determinant yields corrections $\mathcal{O}(n_f/N)$.

The large–N expansion is a powerful tool to explore the strongly interacting regime of gauge theories, and recent developments in string theory have provided beautiful insights in our understanding of the planar limit through the gauge-gravity correspondence [3] (see [4] for an introductory review of recent developments). The lattice formulation of gauge theories allows one to study the non-perturbative dynamics from first principles by numerical simulations, and can therefore be used to investigate how the $N = \infty$ limit is approached. A number of studies in recent years [5, 6, 7, 8, 9, 10, 11] have analyzed in detail several features of pure gauge theories for $N \geq 2$, including the spectrum of glueballs, the k-string tension, and

topology, both at zero and finite temperature. A very precocious scaling has been observed for all observables that have been considered so far, with $1/N^2$ corrections being able to accommodate the values of the observables already for $N = 3$ and in most of the cases also for $N = 2$.

The convergence to the large–N limit for theories with fermions could also be addressed by dynamical simulations. The contributions of the fermionic determinant should increase the size of the corrections, as pointed out above. An intermediate step at a lesser computational cost is the study of properties of mesons and baryons in theories with quenched fermions. Note that since the fermionic determinant is suppressed in the large–N limit, simulations in the quenched approximation should converge to the same limit as in the theory with dynamical fermions, but with corrections $\mathcal{O}(1/N^2)$.

This paper focuses on the low–lying states of the mesonic spectrum for SU(N) theories in the quenched approximation and $N = 2, 3, 4, 6$. By generalizing the lattice Dirac operator to handle spinors of arbitrary dimension in color space, we compute two-point functions for Wilson fermions at one value of the lattice spacing and several values of the bare quark mass. The mass dependence of the spectrum is studied, and extrapolated to the large–N limit. Our results are consistent with a $1/N^2$ scaling, and the results for $N = \infty$ can be used as an input for analytical approaches that study the meson spectrum of strongly–interacting gauge theories.

We stress that this calculation is meant to be exploratory, trying to favor a first overall physical picture over more formal and technical points. A more detailed calculation is currently in progress and will be reported elsewhere.

The paper is organized as follows. Sect. 2 recalls the basic framework that is used for extracting the mesonic spectrum from field correlators in quenched lattice gauge theories and summarizes the choice of bare parameters for each value of N. The numerical results and their analysis are presented in Sect. 3. Finally, we conclude by discussing the large–N extrapolation in Sect. 4 and its relevance for AdS/QCD studies (see [12] for a review) in Sect. 5.

As this work was being completed we noticed that similar problems have been investigated in Ref. [13]. The preliminary results presented there are obtained on slightly smaller lattices (in physical units) with a finer lattice spacing. The two sets of data are complementary and in qualitative agreement. Future calculations will hopefully achieve precise continuum results for the large–N limit of the mesonic spectrum.

2. Lattice formulation

A Monte Carlo ensemble of gauge fields is generated using the Wilson formulation

of pure $\mathrm{SU}(N)$ gauge theory on the lattice, defined by the plaquette action

$$S = -\frac{\beta}{2N} \sum_{x, \mu > \nu} \mathrm{Tr}\left[U(x, \mu) U(x + \mu, \nu) U^\dagger(x + \nu, \mu) U^\dagger(x, \nu) + \mathrm{h.c.} \right] \ , \qquad (2.1)$$

where $U(x, \mu) \in \mathrm{SU}(N)$ are the link variables. The link variables are updated using a Cabibbo–Marinari algorithm [14], where each $\mathrm{SU}(2)$ subgroup of $\mathrm{SU}(N)$ is updated in turn. We have alternated microcanonical and heat–bath steps in a ratio 4:1. We call *sweep* the sequence of four microcanonical and one heat–bath update.

The action of the massive Dirac operator on a generic spinor field $\phi(x)$ is:

$$\begin{aligned}
D_m \phi(x) &= (D + m)\phi(x) \\
&= -\frac{1}{2} \left\{ \sum_\mu \left[(1 - \gamma_\mu) U(x, \mu) \phi(x + \mu) + (1 + \gamma_\mu) U(x - \mu, \mu)^\dagger \phi(x - \mu) \right] - \right. \\
&\qquad \left. - (8 + 2m)\phi(x) \right\} .
\end{aligned} \qquad (2.2)$$

The bare mass is related to the hopping parameter used in the actual simulations by

$$1/(2\kappa) = 4 + m \ . \qquad (2.3)$$

The complete set of bare parameters used in our simulations is summarized in Tab. 1. For this preliminary study we have run simulations for values of N ranging from 2 to 6 at one value of the lattice spacing only. The values of β have been chosen in such a way that the lattice spacing is constant across the various N. More in detail, at each N we chose the critical value of β for the deconfinement phase transition at $N_t = 5$ [7]. To set the scale, another physical quantity (like e.g. the string tension) can be used. Since different quantities have different large–N corrections, a different choice for the scale will affect the size of the $1/N^2$ corrections, but not the $N = \infty$ value. Using the value $T_c = 270$ MeV, for the lattice spacing a we get $a \simeq 0.145$ fm. For our simulations, we used a $N_s^3 \times N_t$ lattice with the spatial size $N_s = 16$ (which corresponds to about 2.3 fm) and the temporal size $N_t = 32$ (about 4.6 fm in physical units). For the quark masses used in this work, our calculation should be free from noticeable finite size effects. For the fermion fields we used periodic boundary conditions in the spatial directions and antiperiodic boundary conditions in the temporal direction. For the gauge field we used periodic boundary conditions in all directions.

We have performed a chiral extrapolation using data from meson correlators at five values of κ for each N. The choice of values for κ relies on previous experience with $\mathrm{SU}(3)$ simulations to yield pseudoscalar meson masses ≥ 450 MeV. The same values of κ have been used for all values of $N \geq 3$, while for $\mathrm{SU}(2)$ a different choice turned out to be necessary, since all κ's but the lowest one were lower than κ_c. Because of the different additive renormalization, these values of κ yield different values for the bare PCAC mass as N is varied.

N	β	κ
2	2.3715	0.156, 0.155, 0.154, 0.153, 0.152
3	5.8000	0.161, 0.160, 0.159, 0.1575, 0.156
4	10.6370	0.161, 0.160, 0.159, 0.1575, 0.156
6	24.5140	0.161, 0.160, 0.159, 0.1575, 0.156

Table 1: Bare parameters used in our simulations.

The mesonic spectrum is extracted from the zero-momentum two-point correlators of quark bilinears with the quantum numbers required to interpolate between a meson state and the vacuum. Let Γ_1 and Γ_2 be two generic products of Dirac γ matrices, a two-point correlator is defined as

$$C_{\Gamma_1,\Gamma_2}(t) = \sum_{\mathbf{x}} \left\langle (\bar{u}\Gamma_1 d)^\dagger (t,\mathbf{x}) (\bar{u}\Gamma_2 d)(0) \right\rangle , \qquad (2.4)$$

where u and d are the fields corresponding to two different quark flavors, which from now on we take to be mass degenerate. All possible choices for the non-singlet quark bilinears and the quantum numbers of the corresponding physical states are summarized in Tab. 2.

Particle	a_0	π	ρ	a_1	b_1
Bilinear	$\bar{u}d$	$\bar{u}\gamma_5 d, \bar{u}\gamma_0\gamma_5 d$	$\bar{u}\gamma_i d, \bar{u}\gamma_0\gamma_i d$	$\bar{u}\gamma_5\gamma_i d$	$\bar{u}\gamma_i\gamma_j d$
J^{PC}	0^{++}	0^{-+}	1^{--}	1^{++}	1^{+-}

Table 2: Bilinear operators for the computation of non-singlet meson masses.

Performing the Wick contractions we can rewrite $C_{\Gamma_1,\Gamma_2}(t)$ in terms of the quark propagator $G(x,y) = (D_m)^{-1}(x,y)$ or, equivalently, of its hermitean version $H(x,y) = G(x,y)\gamma_5$:

$$C_{\Gamma_1,\Gamma_2}(t) = -\sum_{\mathbf{x}} \left\langle \mathrm{tr}\left[\gamma_0 \Gamma_1^\dagger \gamma_0 G(x,0) \Gamma_2 \gamma_5 G(x,0)^\dagger \gamma_5 \right] \right\rangle =$$

$$= -\sum_{\mathbf{x}} \left\langle \mathrm{tr}\left[\gamma_0 \Gamma_1^\dagger \gamma_0 H(x,0) \gamma_5 \Gamma_2 H(x,0) \gamma_5 \right] \right\rangle , \qquad (2.5)$$

(tr indicates the trace over spinor and color indices).

The propagator $G(x,0)_{AB}$ is obtained by inverting the Dirac operator D_m over point sources (capital roman letters $A, B, \dots$ are used for collective indices over spin and color):

$$G(x,0)_{AB} = (D_m)^{-1}_{AC}(x,y)\delta_{CB}\delta_{y,0} = (D_m)^{-1}_{AC}(x,y)\eta_C^{(B)}(y) , \qquad (2.6)$$

where the second equality defines the $4N$ point sources $\eta^{(B)}$.

The algorithm used for the inversion in Eq. (2.6), is a multishift QMR. This enables us to compute all the quark propagators corresponding to different masses simultaneously. We use a version of the QMR suitable for γ_5-hermitean matrices with even-odd preconditioning of the Dirac matrix [15]. In the rare cases when the algorithm fails to converge, we continue the search for a solution using the MINRES algorithm, which is guaranteed to converge, on the hermitean version of the Dirac operator. For all the inversions we required a relative precision of 10^{-5}. To this accuracy, and for the parameters given above, the number of required applications of the Dirac operator to compute the propagator $G(x,0)_{AB}$ at fixed values for the hopping parameters κ is found to become independent of N. We found that the average number of applications of the Dirac matrix required is about 7500, 5000, 5000 for $N = 3, 4, 6$ respectively (for SU(2) we used different parameters).

From general large–N arguments, we expect the occurrence of exceptional configurations to be suppressed as N increases. This is confirmed by preliminary results reported in Ref. [13]. At the values of the parameters we have simulated, there is no sign of the presence of exceptional configurations.

Simulations have been performed with a bespoke code, which has been tested against published results for SU(3) (see [16] for a review of the literature). We have collected 100 configurations for each value of N, separated by 50 Monte Carlo sweeps.

3. Numerical results

3.1 Extracting masses from correlators

Masses can be extracted from the large–t behavior of $C_{\Gamma,\Gamma}(t)$. Inserting the energy eigenstates in the RHS of Eq. (2.4) yields

$$C_{\Gamma,\Gamma}(t) = \sum_i |c_i|^2 e^{-m_i t} , \tag{3.1}$$

where $c_i = (1/2m_i) \langle 0 | (\bar{u}\Gamma d)(0)| i \rangle$, Γ is one of the γ matrix products appearing in the bilinears in Tab. 2, $|i\rangle$ is an eigenstate of the Hamiltonian with the same quantum numbers as the fermion bilinear, and m_i is the mass of the $|i\rangle$ eigenstate. In the limit $t \to \infty$, the previous equation becomes

$$C_{\Gamma,\Gamma}(t) \underset{t\to\infty}{=} |c_0|^2 e^{-m_0 t} , \tag{3.2}$$

i.e. at large time correlation functions decay in time as a single exponential with a typical time given by the inverse mass of the lowest-lying state in the spectrum with matching quantum numbers. The lowest mass in a given channel can then be extracted as

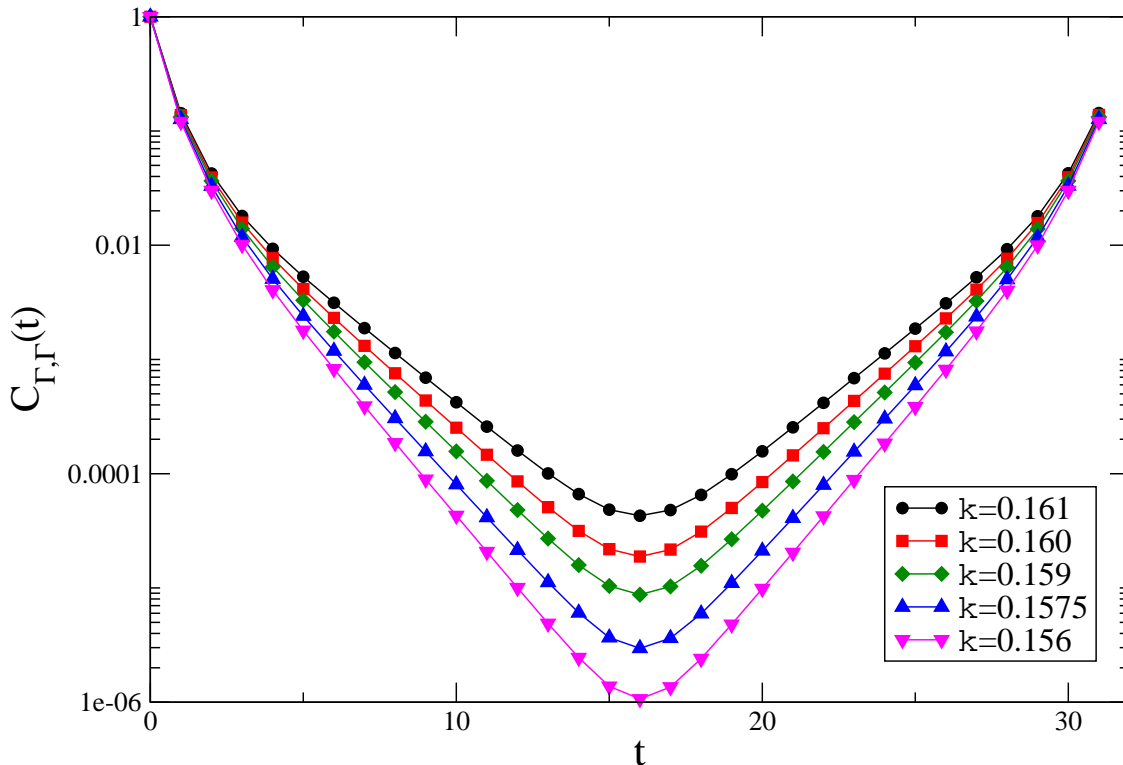$$m_0 = - \lim_{t\to\infty} \frac{\log C_{\Gamma,\Gamma}(t)}{t} . \tag{3.3}$$

Figure 1: Correlators for SU(4) and $\Gamma = \gamma_5$ at the values of κ shown. The correlators have been normalized in such a way that at $t = 0$ their value is 1. The lines joining the data are only guides for the eyes.

Practically, one defines the effective mass $m_0(t)$ as

$$m_0(t) = -\log \frac{C_{\Gamma,\Gamma}(t)}{C_{\Gamma,\Gamma}(t-1)} \tag{3.4}$$

and obtains m_0 by fitting $m_0(t)$ to a constant at large enough t.

On a finite lattice the exponential in the large–time behavior of the propagator is replaced by a cosh and an effective mass can be defined as

$$m_0(t) = \text{acosh}\left(\frac{C_{\Gamma,\Gamma}(t+1) + C_{\Gamma,\Gamma}(t-1)}{2C_{\Gamma,\Gamma}(t)}\right) . \tag{3.5}$$

Typical examples of correlation functions and effective masses as a function of the separation between source and sink are shown respectively in Fig. 1 and Fig. 2.

We have estimated the errors on the correlators using a jack-knife method, and checked that the bootstrap method gives similar results. With simple link operators, we have been able to extract an unambiguous signal for the π and the ρ mesons (to which we limit our analysis). Other correlators yielded a noisy signal, and we plan to investigate the possibility of improving the signal-to-noise ratio by more sophisticated
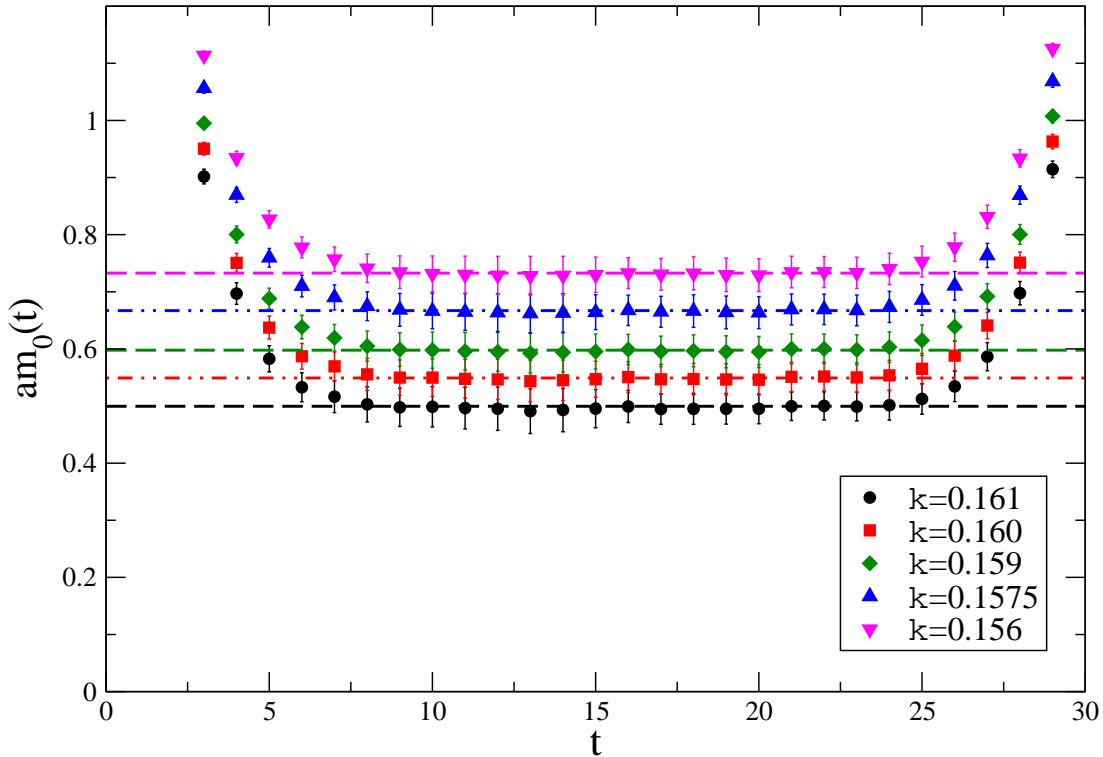
Figure 2: Effective masses from the correlators in Fig. 1. The straight lines are fits to the data at plateau.

measurements. Due to the small number of data points, often correlated fits proved to be unreliable, as already observed (see e.g. Refs. [17, 18]). Hence, masses have been extracted with uncorrelated fits and the error estimated with a jack-knife procedure. We have checked that the uncorrelated fit results coincide with the correlated fit results whenever the correlated fits give reasonable values for the parameters and the χ^2.

Our results for the various N for the PCAC mass m_{PCAC}, the mass of the pion m_π, and the mass of the ρ m_ρ are reported in Tabs. 3–6. The details of our analysis are explained in the following two subsections.

In order to convert the results expressed in lattice units to masses in physical units, we note that

$$am = (aT_c)(m/T_c) = m/(5T_c) \tag{3.6}$$

(the last equality uses the fact that the lattice spacing has been fixed in such a way that the deconfinement phase transition corresponds to $N_t = 5$). As a reference scale, we can use T_c for SU(3), which is approximately 270 MeV.

3.2 Meson masses at finite N

The pion is the would-be Goldstone boson of chiral symmetry breaking. Chiral

κ	$am_{\rm PCAC}$	$m_{\rm PCAC}$ (MeV)	am_π	m_π (MeV)	am_ρ	m_ρ (MeV)
0.152	0.0824(30)	111(4)	0.541(3)	730(4)	0.620(6)	837(8)
0.153	0.0669(28)	90(4)	0.492(4)	664(5)	0.584(7)	788(9)
0.154	0.0522(25)	70(3)	0.441(4)	595(5)	0.547(7)	738(9)
0.155	0.0396(24)	53(3)	0.389(4)	525(5)	0.510(10)	789(13)
0.156	0.0261(22)	35(3)	0.319(7)	430(9)	0.458(17)	618(23)

Table 3: Numerical results for SU(2). Masses in lattice units have been converted to physical units by noting $a = 1/(5T_c)$.

κ	$am_{\rm PCAC}$	$m_{\rm PCAC}$ (MeV)	am_π	m_π (MeV)	am_ρ	m_ρ (MeV)
0.156	0.1047(24)	141(3)	0.625(2)	844(3)	0.720(3)	972(4)
0.1575	0.0797(21)	108(3)	0.553(2)	747(3)	0.667(4)	900(5)
0.159	0.0574(17)	77(2)	0.476(2)	643(3)	0.616(5)	832(7)
0.160	0.0431(16)	58(2)	0.420(2)	567(3)	0.582(6)	786(8)
0.161	0.0299(14)	40(2)	0.362(3)	489(4)	0.550(7)	743(9)

Table 4: Numerical results for SU(3). Masses in lattice units have been converted to physical units by noting $a = 1/(5T_c)$.

κ	$am_{\rm PCAC}$	$m_{\rm PCAC}$ (MeV)	am_π	m_π (MeV)	am_ρ	m_ρ (MeV)
0.156	0.1506(35)	203(5)	0.733(1)	990(1)	0.817(2)	1103(3)
0.1575	0.1234(29)	167(4)	0.667(1)	900(1)	0.766(2)	1034(3)
0.159	0.0981(22)	132(3)	0.598(1)	807(1)	0.714(2)	964(3)
0.160	0.0817(19)	110(3)	0.549(2)	741(3)	0.680(2)	918(3)
0.161	0.0659(17)	89(2)	0.499(2)	674(3)	0.646(3)	872(4)

Table 5: Numerical results for SU(4). Masses in lattice units have been converted to physical units by noting $a = 1/(5T_c)$.

perturbation theory at leading order predicts

$$m_\pi = A \left(\frac{1}{\kappa} - \frac{1}{\kappa_c} \right)^{1/2} . \tag{3.7}$$

Hence the value of κ corresponding to the chiral limit, κ_c, can be obtained by fitting the pion mass according to Eq. (3.7). Eq. (3.7) is modified for the quenched theory, where quenched chiral logs appear. For quenched SU(N) gauge theory we expect

$$m_\pi = A \left(\frac{1}{\kappa} - \frac{1}{\kappa_c} \right)^{1/[2(1+\delta)]} , \tag{3.8}$$

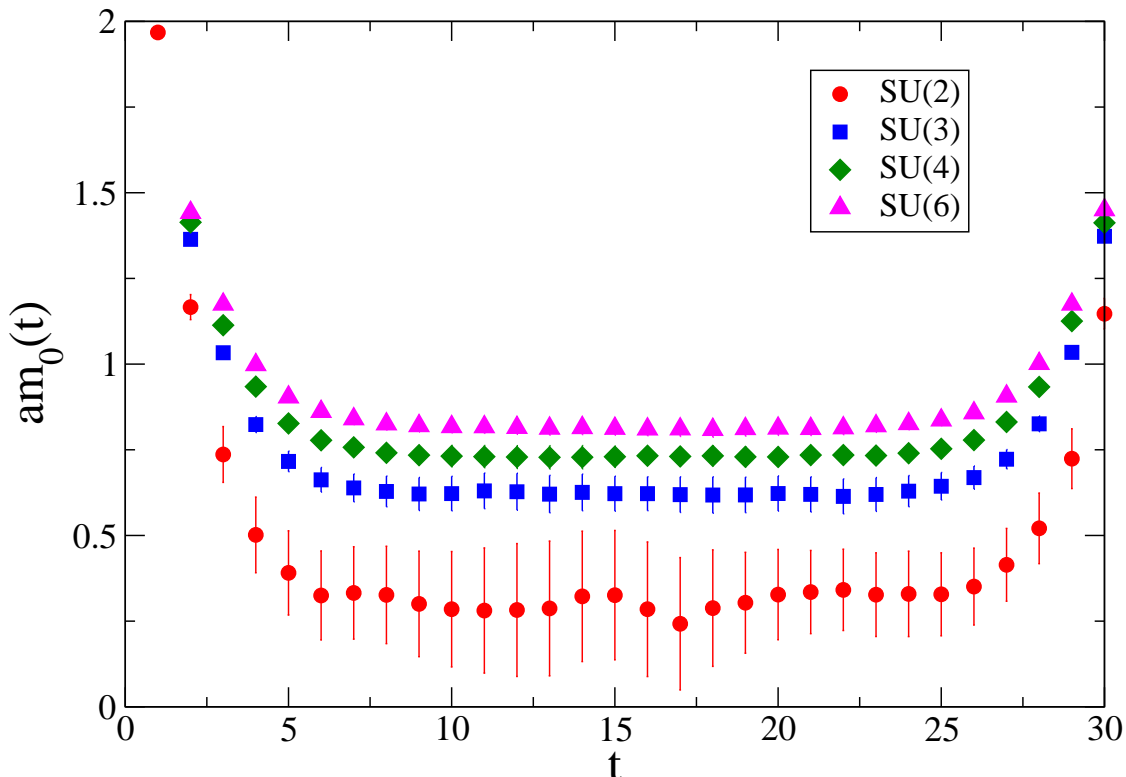where δ is positive, $\mathcal{O}(10^{-1})$ for SU(3) and goes like $1/N$ [19].

Figure 3: Effective masses from C_{γ_5,γ_5} at $\kappa = 0.156$.

κ	am_{PCAC}	m_{PCAC} (MeV)	am_π	m_π (MeV)	am_ρ	m_ρ (MeV)
0.156	0.1789(22)	241(3)	0.814(1)	1099(1)	0.889(2)	1214(3)
0.1575	0.1509(20)	203(3)	0.752(1)	1015(1)	0.838(2)	1131(3)
0.159	0.1248(18)	168(2)	0.687(1)	927(1)	0.786(2)	1061(3)
0.160	0.1078(17)	146(2)	0.6425(9)	867(1)	0.752(2)	1015(3)
0.161	0.0914(15)	123(2)	0.5952(9)	804(1)	0.718(2)	969(3)

Table 6: Numerical results for SU(6). Masses in lattice units have been converted to physical units by noting $a = 1/(5T_c)$.

The mass of the pion can be extracted by looking at correlators $C_{\Gamma,\Gamma}$ in which Γ is either γ_5 or $\gamma_0\gamma_5$. In the latter case, it was not possible to extract a signal for all κ's in SU(2). Hence, although in general mass plateau fits of $\gamma_0\gamma_5$ have a lower χ^2, we will mostly focus on numerical results obtained with $\Gamma = \gamma_5$.

As N grows, so does m_π at fixed κ. A plot comparing numerical results for the effective mass extracted from C_{γ_5,γ_5} is shown in Fig. 3. A linear fit to the data according to Eq. (3.7) enables us to extract the critical values of κ for the N at which we have simulated. Results are shown in Tab. 7. The mass obtained from the

N	κ_c	A
2	0.15827(12)	1.0583(99)
3	0.16359(28)	1.142(21)
4	0.16556(23)	1.201(14)
6	0.16716(12)	1.2422(69)

Table 7: Fitted values for κ_c and A at various N.

$C_{\gamma_0\gamma_5,\gamma_0\gamma_5}$ correlator yields compatible results. Higher statistics and a careful study of the systematics are necessary for a more precise determination of the critical value of κ.

Generally the reduced χ^2 of the fits according to Eq. (3.7) varies between two and four. One can check whether this relatively high value of χ_r^2 is due to the fact that we are neglecting chiral logarithms. For $N \geq 2$, fits according to (3.8) yield a value of χ_r^2 that is below one, but δ is found to be negative. This agrees with the findings of [16], where the negative value is interpreted as a consequence of simulating far from the chiral limit. In fact, for $N = 2$, where we have the lightest pion mass, δ is found to be compatible with zero. As one would have expected, for $m_\pi \geq 450$ MeV there is no sensitivity to the chiral logarithms [19]. Instead of relying on phenomenological fits like in [16], we acknowledge the impossibility to determine δ and neglect the chiral logarithms, using the chiral behavior (3.8) to get an estimate for the systematic error associated with this approximation. For SU(2), the three-parameter fit gives a value of κ_c that is higher than the fit with $\delta = 0$ by about 1%. Considering that $\delta \propto N^{-1}$, a conservative but safe estimate for the systematic error associated with the chiral logarithms is of the order of a few percent. This is in agreement with the literature for SU(3) [16]. We will come back on issues associated with the chiral logarithms in the next subsection.

The mass of the ρ has been extracted from C_{γ_i,γ_i}, after taking the average over the spatial direction i of the correlation functions. Fits in the $C_{\gamma_0\gamma_i,\gamma_0\gamma_i}$ channel also yield compatible results.

At small quark mass, m_ρ depends linearly on the quark mass and goes to a finite value in the chiral limit. Using Eq. (3.7), this can be rephrased into the following relationship between m_ρ and m_π

$$m_\rho = m_\rho^\chi + B m_\pi^2 \ , \tag{3.9}$$

where m_ρ^χ is the mass of the ρ meson at the chiral point. Note that the previous equation is not modified by chiral logarithms [19]. Assuming that Eq. (3.9) holds in our case[1], we can fit m_ρ^χ and B at the various values of N from our data. Our results

---

[1]More sophisticated dependencies (e.g. the addition of a linear term in m_π to Eq. (3.9), which is motivated by phenomenology) are also supported by our data. In the absence of any evidence against it, we chose to fit the parameters using the simple chiral functional behavior.

N	am_ρ^χ	B
2	0.3890(75)	0.797(31)
3	0.4683(25)	0.6455(84)
4	0.5018(36)	0.5905(88)
6	0.5238(40)	0.5533(77)

Table 8: Extrapolation of m_ρ to the chiral limit.

for those quantities are reported in Tab. 8. The reduced χ^2 of the fits (which keep into account both the error on m_ρ and the error on m_π) is always less than one.

3.3 PCAC

As noted in the previous subsection, Eq. (3.7) only holds for the full theory, while it is modified at small masses, where quenched chiral logs become important. An alternative way of defining κ_c, which is free from these ambiguities, makes use of the partially conserved axial current (PCAC) relation. In the continuum, the PCAC relation reads

$$\partial_\mu A^\mu(x) = 2m_{\mathrm{PCAC}} j(x) \ , \tag{3.10}$$

with $A^\mu(x) = \bar{u}(x)\gamma_\mu\gamma_5 d(x)$ and $j = \bar{u}(x)\gamma_5 d(x)$. The previous equation allows us to determine m_{PCAC} as

$$m_{\mathrm{PCAC}} = \frac{1}{2}\frac{\langle \int \mathrm{d}\vec{x}(\partial_0 A^0(x)) j^\dagger(y))\rangle}{\langle \int \mathrm{d}\vec{x} j(x) j^\dagger(y)\rangle} \ , \tag{3.11}$$

where y is an arbitrary point. On the lattice an effective mass $m_{\mathrm{PCAC}}(t)$ can be defined as

$$m_{\mathrm{PCAC}}(t) = \frac{1}{4}\frac{C_{\gamma_0\gamma_5,\gamma_5}(t+1) - C_{\gamma_0\gamma_5,\gamma_5}(t-1)}{C_{\gamma_5,\gamma_5}(t)} \tag{3.12}$$

and once again fitted at plateau. Note that with our choice for the discretized fermions PCAC holds on the lattice up to terms $\mathcal{O}(a)$. In practice, since $m_{\mathrm{PCAC}}(t)$ defined through Eq. (3.12) is antisymmetric around the point $N_t/2$, one averages the absolute values at points t and $N_t - t$. An example of an effective mass plateau obtained using Eq. (3.12) is given in Fig. 4.

Since $m_{\mathrm{PCAC}} = Z_m(1/\kappa - 1/\kappa_c)$, we can determine κ_c as the value for which $m_{\mathrm{PCAC}} = 0$. A linear fit to the data enables us to extract κ_c. Results for $N = 2, 3, 4, 6$ are reported in Tab. 9. Comparing with the similar fits from m_π (Tab. 7), it is immediate to see that using m_{PCAC} we get values for κ_c that are systematically lower[2]. Although this effect is below half a percent, it is by far larger than the

---

[2]This should be contrasted with fits that keep into account chiral logarithms, for which we find values of κ_c systematically higher.

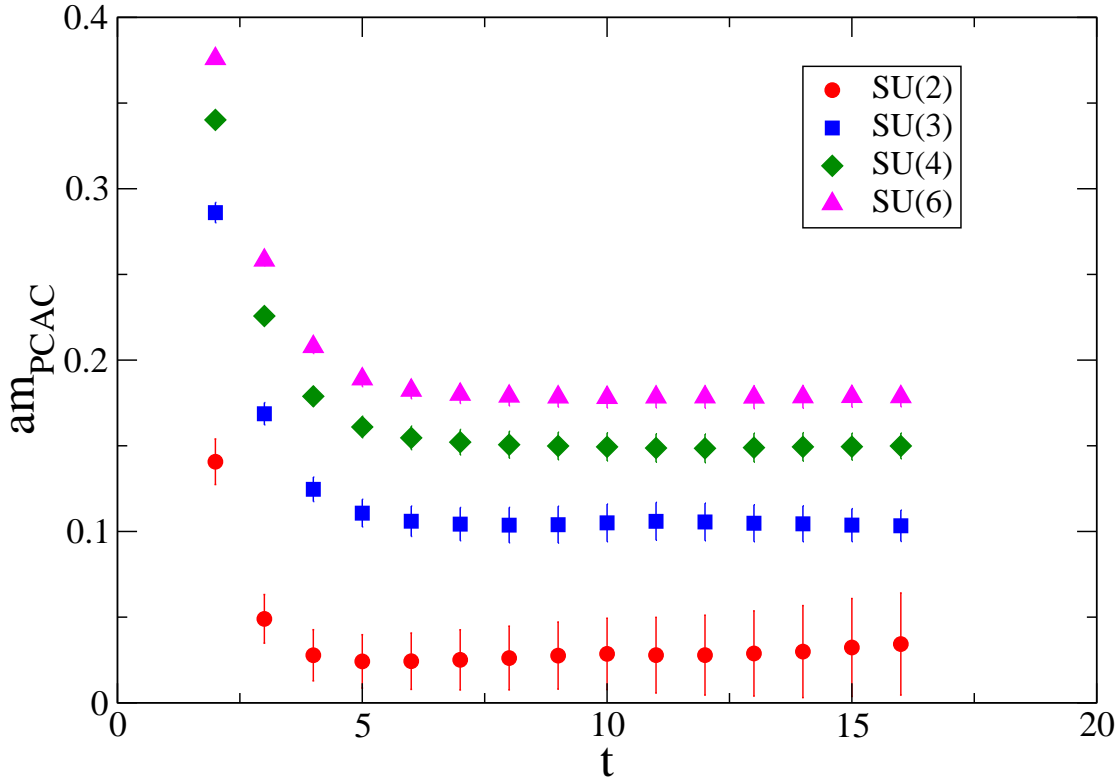**Figure 4:** $m_{\mathrm{PCAC}}(t)$ as a function of t for $\kappa = 0.156$.

N	κ_c	A
2	0.15792(25)	0.331(15)
3	0.16306(10)	0.372(10)
4	0.16513(15)	0.422(12)
6	0.16657(15)	0.438(11)

Table 9: Extrapolation of κ to the chiral limit using m_{PCAC}.

statistical errors. This discrepancy might be due to the different chiral behavior of the two definitions of the quark mass for the quenched theory or be a consequence of the underestimation of the errors due to the use of uncorrelated fits, as we have discussed above. However, at our value of the lattice spacing discretization errors also play a relevant part. In order to investigate these issues, we have analyzed m_{π} as a function of m_{PCAC}. Our results are reported in Fig. 5, where m_{π} is plotted as a function of m_{PCAC}.

The expected quadratic behavior

$$m_{\pi}^2 = C m_{\mathrm{PCAC}} \tag{3.13}$$

is not obeyed by our data. To extrapolate to the chiral limit, we need to correct the
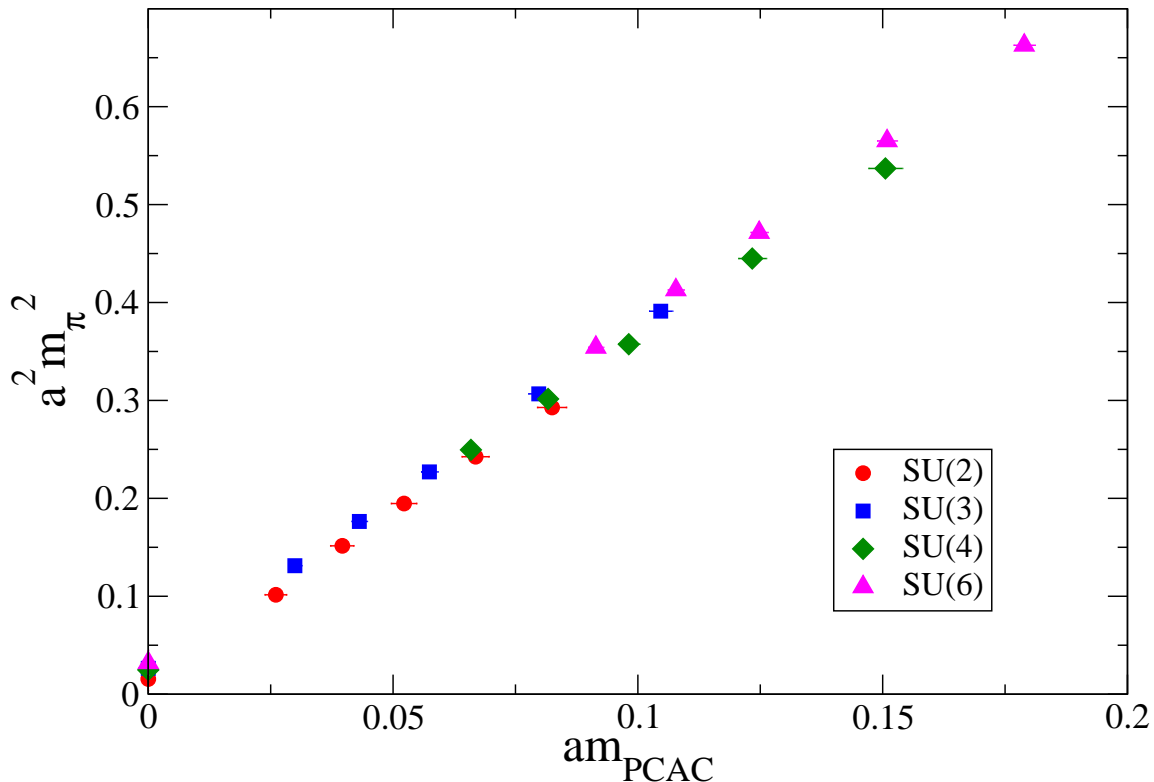
Figure 5: m_π^2 as a function of m_{PCAC} at the various N. The values of m_π at $m_{\mathrm{PCAC}} = 0$ have been obtained with a linear fit to the data, as discussed in the text.

above relationship by allowing for a non-zero value for m_π when m_{PCAC} is zero:

$$m_\pi^2 = Cm_{\mathrm{PCAC}} + B \ , \tag{3.14}$$

where B and C depend on N. B (obtained from a fit according to the previous equation keeping into account both the errors on m_π and on m_{PCAC}) is roughly of order 10^{-2} and independent of N. If the existence of a constant (as a function of N) residual m_π as $m \to 0$ were a sign of the failure of the quenched approximation, we would have expected B to go to zero as $N \to \infty$. This expectation is not supported by our data. On the other hand, having fixed the lattice spacing across the gauge groups, any discretization artifact would be constant in N. Hence, it is likely that this residual mass is (mostly) due to the violation of PCAC on the lattice. If this is correct, also the systematic discrepancy between the two sets of κ_c should be due to lattice artifacts. In order to settle this issue, a systematic study at different lattice spacings needs to be performed.

4. Extrapolation to $SU(\infty)$

Using data at finite N, we can estimate the behavior of the lowest-lying meson masses

at $N = \infty$. Following similar analysis performed in pure gauge [5, 6, 7, 8, 9, 10, 11], we use predictions from the large–N expansion to see whether they hold in the non-perturbative regime. In practice, we take the asymptotic expansion for an observable O in the quenched case [1]

$$O(N) = O(\infty) + \sum_i \frac{\alpha_i}{N^{2i}} \tag{4.1}$$

and we check whether a reasonable (as dictated by the number of data) truncation of this series accommodates our numerical values. In the pure gauge case, a preco-cious onset of the large–N behavior has been found for all the observables that have been studied (which include glueball masses, deconfining temperature and topolog-ical susceptibility): the $\mathcal{O}(1/N^2)$ correction correctly describes the data down to at least $N = 3$, often including also the case $N = 2$. From a qualitative point of view, it is already clear from what we have seen so far that the quantities we have investi-gated have a mild dependence on N. In this section, we want to study whether this dependence is correctly described by a large–N-inspired expansion.

κ_c can be computed in lattice perturbation theory [20]. The result at one loop is in agreement with the predictions of the large–N limit: this quantity receives a correction $\mathcal{O}(1/N^2)$. This motivates the fit

$$\kappa_c(N) = \kappa_c(\infty) + \frac{a}{N^2} \ . \tag{4.2}$$

For κ_c obtained via Eq. (3.7), we get $\kappa_c(\infty) = 0.1682(1)$ and $a = -0.0398(6)$, with $\chi_r^2 = 0.6$. The quality of the fit is good, and the coefficient of the $1/N^2$ correction is small, as one would expect for a series expansion. Similarly to the pure gauge case, we observe an early onset of the asymptotic behavior, which captures also the SU(2) value. Our data and the large–N extrapolation are plotted in Fig. 6. The same extrapolation for the critical value of κ obtained using the PCAC relation yields $\kappa_c(\infty) = 0.1675(2)$, $a = -0.039(1)$ and $\chi_r^2 = 1.3$. The discrepancy between the values of $\kappa_c(\infty)$ could be due to lattice discretization artifacts, as discussed in Sect. 3.3. We take the difference between the two determinations should be seen as an estimate of the systematic error. The fact that the angular coefficient a has the same value seems to corroborate this hypothesis. A more precise determination of κ_c is beyond the scope of this work.

The slope A in Eq. (3.7) can also be extrapolated to the $N = \infty$ limit, with corrections that are $\mathcal{O}(1/N^2)$:

$$A(N) = A(\infty) + a/N^2 \ . \tag{4.3}$$

For the C_{γ_5, γ_5} results, the fit gives $A(\infty) = 1.262(8)$ and $a = -0.82(6)$ with $\chi_r^2 = 1.2$. This allows us to write the mass of the π as a function of κ at $N = \infty$ as

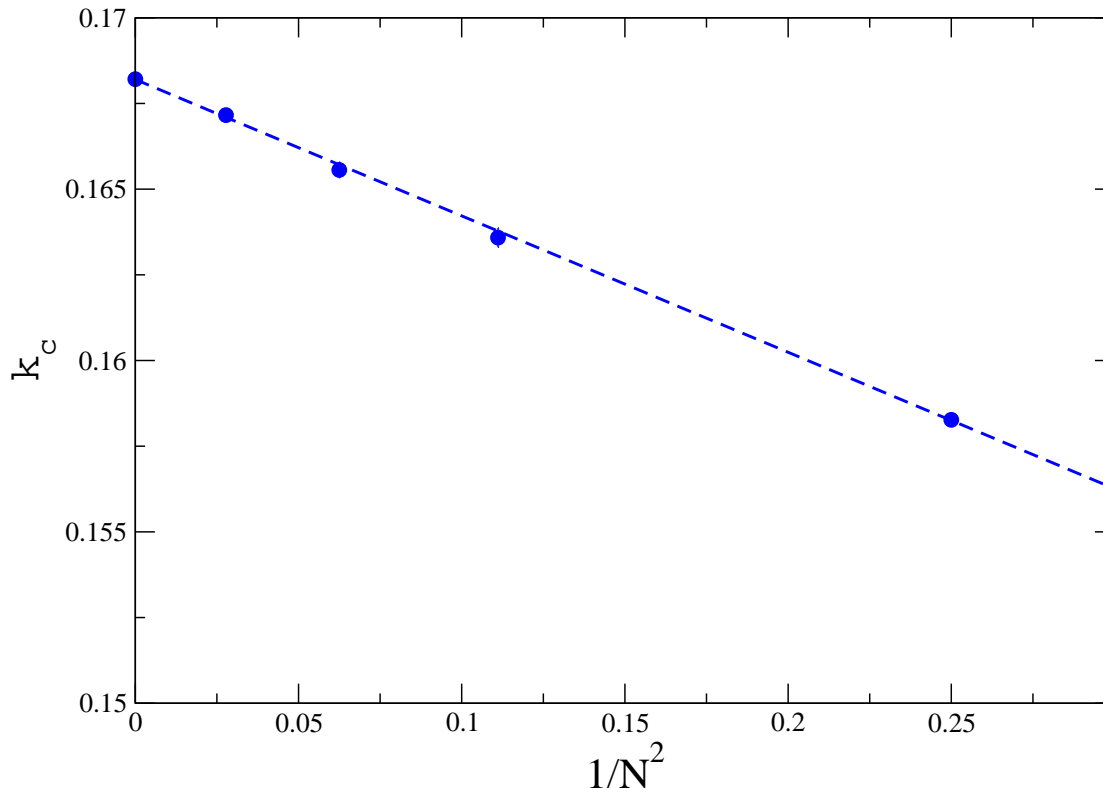$$m_\pi = 1.262(8) \, (1/\kappa - 5.945(4))^{1/2} \ , \tag{4.4}$$

Figure 6: Extrapolation of κ_c to $N = \infty$.

where the values of κ_c obtained from fits to C_{γ_5,γ_5} have been used (using the PCAC value gives a slightly discrepant result, for the reasons discussed in Sect. 3.3). We plot in Fig. 7 the data for the dependence of m_π^2 as a function of κ, with a fit according to Eq. (3.7). We also plot in the same figure Eq. (4.4).

The parameters describing m_ρ as a function of m_π (Eq. (3.9)) are also expected to follow the asymptotic expansion (4.1). A fit with only the leading $1/N^2$ correction yields

$$
\begin{aligned}
m_\rho^\chi(N) &= 0.539(3) - 0.62(3)/N^2 \ , & \chi_r^2 &= 0.008 \ ; \\
B(N) &= 0.5224(8) + 1.10(1)/N^2 \ , & \chi_r^2 &= 0.7 \ .
\end{aligned}
\tag{4.5}
$$

The tiny χ_r^2 for $B(\infty)$ is particularly surprising, given the statistical independence of the measured values of $B(N)$. We see that once again the leading behavior describes very well the parameters and that the coefficient of the $1/N^2$ correction is order one.

As a result of this analysis, at $N = \infty$ we can describe m_ρ as a function of m_π as

$$
m_\rho = 0.539(3) + 0.5224(8)m_\pi^2 \ .
\tag{4.6}
$$

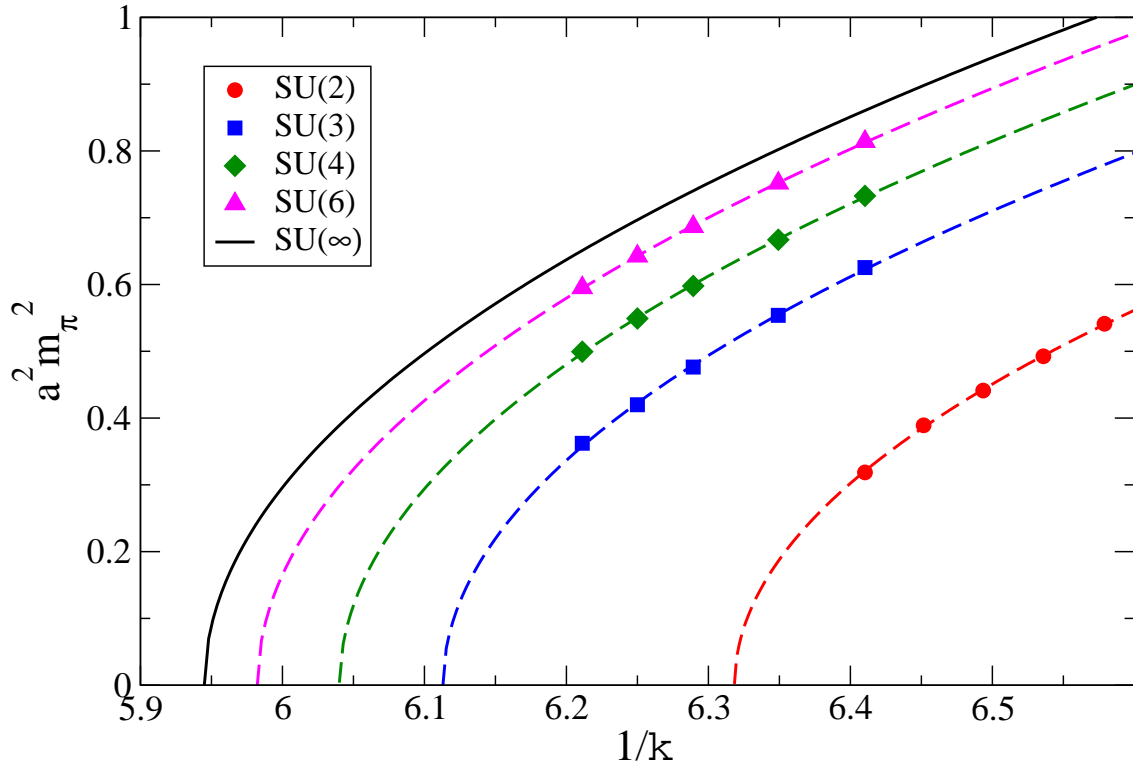This relationship, together with the data and the fits at finite N, is plotted in Fig. 8.

Figure 7: m_π as a function of $1/\kappa$. The curves through the data are obtained from a fit assuming the expected leading dependence from chiral perturbation theory. Also shown is the extrapolation to $N = \infty$.

5. Discussion and conclusions

In this paper, we have used standard lattice QCD methods for computing correlation functions to extract the masses of the ρ and π mesons in the large–N limit of $\mathrm{SU}(N)$ gauge theories. The masses in the limiting theory have been obtained with an extrapolation from the quenched data at $N = 2, 3, 4, 6$ using the large–N behavior deduced from arguments inspired by a diagrammatic expansion. We find that the extrapolation works well in its simplest form, i.e. using only the leading correction to the large–N value. This allows us to determine the behavior at $N = \infty$ of the mass of the pion as a function of the renormalized quark mass and of the mass of the ρ as a function of the mass of the pion (chiral perturbation theory has also been used as an input). The two central results of this paper are summarized by the parametrization

$$m_\pi(N) = \left(1.262(8) - \frac{0.82(6)}{N^2}\right)\left(\frac{1}{\kappa} - 5.945(4) + \frac{0.0398(6)}{N^2}\right)^{1/2} \tag{5.1}$$

and

$$m_\rho(N) = \left(0.539(3) - \frac{0.62(3)}{N^2}\right) + \left(0.5224(8) + \frac{1.10(1)}{N^2}\right) m_\pi^2(N) . \tag{5.2}$$
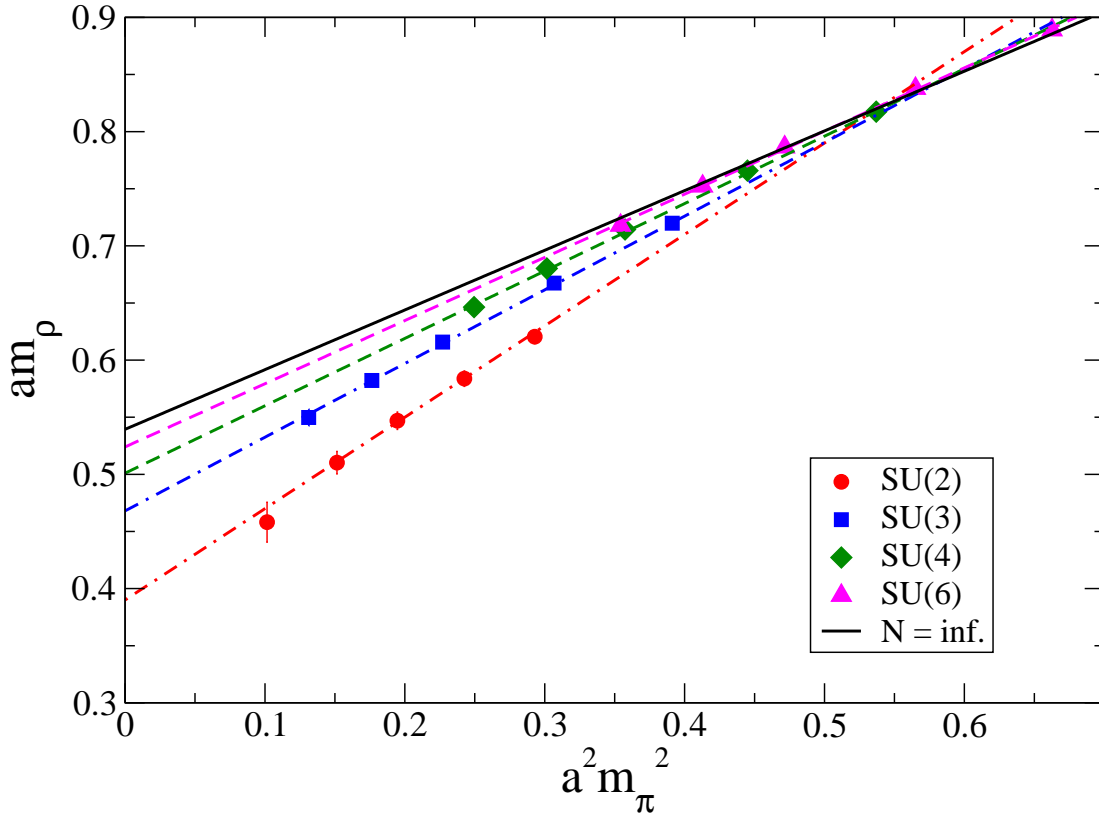
Figure 8: m_ρ vs. m_π. Lines through the data have been obtained with a plot inspired by chiral perturbation theory. Also shown is the extrapolation to $N = \infty$.

One of the motivations to perform a calculation from first principles for the large–N limit of SU(N) gauge theories is to compare with predictions obtained in the AdS/CFT framework. To date, no AdS background has been found that can be considered a good dual description of non-supersymmetric QCD extrapolated at large–N. Hence, one could use our calculation to benchmark the proposed AdS ansatz. From this point of view, we notice a striking agreement with a calculation [21, 12] using the Constable-Myers background [22], which (after normalizing the mass of the ρ in the chiral limit to our data) finds for the coefficient of m_π^2 (see Eq. (3.9)) 0.57. This number is in agreement with our calculations within 5%. However, before we can draw any conclusion from the comparison with the lattice, an extrapolation of the lattice data to the continuum limit is needed.

Beyond the specific numerical details, our calculation seems to indicate that (a) the large–N theory is a well defined theory; (b) lattice calculations can be successfully exploited to compute the parameters of this theory; (c) at least in the quenched theory, to describe results at any finite N only the first term in the expected power series in $1/N^2$ is required; (d) the coefficient of the correction is at most order one, justifying the idea of a power expansion. All these indications are perfectly in line with what we have already learned for the SU(N) theory without fermionic matter.

Although this can be considered obvious, since our calculation is quenched, we stress that the $N = \infty$ limit is also quenched. In other words, to describe the limiting theory a quenched calculation suffices. The inclusion of the full fermion determinant becomes mandatory if one is interested in the actual size of the finite N corrections. In particular, one expects larger corrections ($\mathcal{O}(n_f/N)$) in the unquenched theory.

As we have stressed several times, one of the main limitations of this calculation is that our chiral extrapolations are not sensitive to the expected chiral log behavior. We have conservatively estimated that this approximation produces a 3% systematic error. This error does not affect our conclusions. Moreover, we note that chiral logarithms do not modify Eq. (5.2). In any case, in order to make more robust estimates, better control on the chiral extrapolation should be achieved. This requires simulating at smaller pion masses. It would also be nice to check that the chiral log effects decrease as N increases.

Another source of systematic error in our calculation is the fact that simulations have been performed at one single lattice spacing. For this reason we regard our results as exploratory. As discussed in Sect. 3.3, lattice artifacts do seem to play a role, although they are not big enough to spoil the features of the theory and the way in which the large–N behavior is approached. Nevertheless, a study closer to the continuum is necessary to clarify these issues. Work for the extrapolation to the continuum limit is already in progress. For this extrapolation, the use of an improved fermion action can mitigate the discretization artifacts, decreasing considerably the required numerical effort. We shall explore this possibility in the future. As for finite size effects, we have argued in Sect. 2 that with our choice of parameters they can be neglected, but this also ought to be verified directly.

Aside from technicalities, other features of the large–N theory, like the spectrum in the flavor singlet channel and masses of heavier mesons, also deserve to be investigated. While the latter problem can probably be dealt with using improved techniques for computing correlation functions (e.g. with smeared links replacing straight links and smeared sources replacing point sources), for the scalar mesons, for which disconnected contributions are important, different strategies need to be adopted. An adaptation of the techniques exposed in [23, 24] is in progress. Results will be reported in a future publication.

Acknowledgments

References

[1] G. 't Hooft, *A planar diagram theory for strong interactions*, *Nucl. Phys.* **B72** (1974) 461.

[2] G. Veneziano, *Regge intercepts and unitarity in planar dual models*, *Nucl. Phys.* **B74** (1974) 365.

[3] J. M. Maldacena, *The large n limit of superconformal field theories and supergravity*, *Adv. Theor. Math. Phys.* **2** (1998) 231–252, [`hep-th/9711200`].

[4] H. Nastase, *Introduction to ads-cft*, `0712.0689`.

[5] B. Lucini and M. Teper, *Su(n) gauge theories in four dimensions: Exploring the approach to n = infinity*, *JHEP* **06** (2001) 050, [`hep-lat/0103027`].

[6] B. Lucini, M. Teper, and U. Wenger, *The high temperature phase transition in su(n) gauge theories*, *JHEP* **01** (2004) 061, [`hep-lat/0307017`].

[7] B. Lucini, M. Teper, and U. Wenger, *Topology of su(n) gauge theories at t approx. 0 and t approx. t(c)*, *Nucl. Phys.* **B715** (2005) 461–482, [`hep-lat/0401028`].

[8] L. Del Debbio, H. Panagopoulos, P. Rossi, and E. Vicari, *Spectrum of confining strings in su(n) gauge theories*, *JHEP* **01** (2002) 009, [`hep-th/0111090`].

[9] L. Del Debbio, H. Panagopoulos, and E. Vicari, *Theta dependence of su(n) gauge theories*, *JHEP* **08** (2002) 044, [`hep-th/0204125`].

[10] L. Del Debbio, H. Panagopoulos, and E. Vicari, *Topological susceptibility of su(n) gauge theories at finite temperature*, *JHEP* **09** (2004) 028, [`hep-th/0407068`].

[11] L. Del Debbio, G. M. Manca, H. Panagopoulos, A. Skouroupathis, and E. Vicari, *theta-dependence of the spectrum of su(n) gauge theories*, *JHEP* **06** (2006) 005, [`hep-th/0603041`].

[12] J. Erdmenger, N. Evans, I. Kirsch, and E. Threlfall, *Mesons in gauge/gravity duals - a review*, `0711.4467`.

[13] G. Bali and F. Bursa, *Meson masses at large n_c*, `0708.3427`.

[14] N. Cabibbo and E. Marinari, *A new method for updating su(n) matrices in computer simulations of gauge theories*, *Phys. Lett.* **B119** (1982) 387–390.

[15] A. Frommer, B. Nockel, S. Gusken, T. Lippert, and K. Schilling, *Many masses on one stroke: Economic computation of quark propagators*, *Int. J. Mod. Phys.* **C6** (1995) 627–638, [`hep-lat/9504020`].

[16] M. Gockeler *et. al.*, *Scaling of non-perturbatively o(a) improved wilson fermions: Hadron spectrum, quark masses and decay constants*, *Phys. Rev.* **D57** (1998) 5562–5580, [`hep-lat/9707021`].

[17] C. Michael, *Fitting correlated data*, *Phys. Rev.* **D49** (1994) 2616–2619, [`hep-lat/9310026`].

[18] C. Michael and A. McKerrell, *Fitting correlated hadron mass spectrum data*, *Phys. Rev.* **D51** (1995) 3745–3750, [`hep-lat/9412087`].

[19] S. R. Sharpe, *Quenched chiral logarithms*, *Phys. Rev.* **D46** (1992) 3146–3168, [`hep-lat/9205020`].

[20] J. Stehr and P. H. Weisz, *Note on gauge fixing in lattice qcd*, *Lett. Nuovo Cim.* **37** (1983) 173–177.

[21] J. Babington, J. Erdmenger, N. J. Evans, Z. Guralnik, and I. Kirsch, *Chiral symmetry breaking and pions in non-supersymmetric gauge / gravity duals*, *Phys. Rev.* **D69** (2004) 066007, [`hep-th/0306018`].

[22] N. R. Constable and R. C. Myers, *Exotic scalar states in the ads/cft correspondence*, *JHEP* **11** (1999) 020, [`hep-th/9905081`].

[23] J. Foley *et. al.*, *Practical all-to-all propagators for lattice qcd*, *Comput. Phys. Commun.* **172** (2005) 145–162, [`hep-lat/0505023`].

[24] S. Collins, G. Bali, and A. Schafer, *Disconnected contributions to hadronic structure: a new method for stochastic noise reduction*, `0709.3217`.